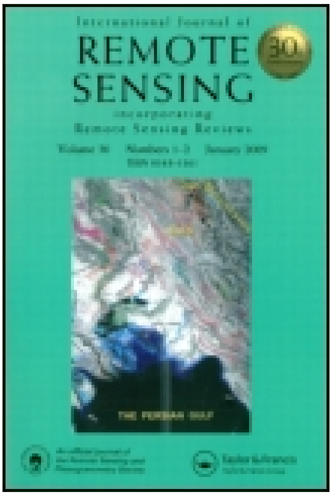

International Journal of Remote Sensing
Publication details, including instructions for authors and subscription information:
http://www.tandfonline.com/loi/tres20

Hyperspectral indices for detecting changes in canopy reflectance as a result of underground natural gas leakage

M. F. Noomen [a] , K. L. Smith [b] , J. J. Colls [b] , M. D. Steven [c] , A. K. Skidmore [a] & F. D. Van Der Meer [a]

[a] International Institute for Geoinformation Science and Earth Observation (ITC) , Enschede, the Netherlands

[b] Division of Agricultural and Environmental Sciences , School of Biosciences , University of Nottingham , UK

[c] School of Geography , University of Nottingham , UK

Published online: 20 Sep 2008.

International Journal of Remote Sensing
Vol. 29, No. 20, 20 October 2008, 5987–6008

Hyperspectral indices for detecting changes in canopy reflectance as a result of underground natural gas leakage

M. F. NOOMEN*†, K. L. SMITH‡, J. J. COLLS‡, M. D. STEVEN§, A. K. SKIDMORE† and F. D. VAN DER MEER†

†International Institute for Geoinformation Science and Earth Observation (ITC), Enschede, the Netherlands

‡Division of Agricultural and Environmental Sciences, School of Biosciences, University of Nottingham, UK

§School of Geography, University of Nottingham, UK

(*Received 5 August 2006; in final form 15 January 2008*)

Natural gas leakage from underground pipelines is known to affect vegetation adversely, probably by displacement of the soil oxygen needed for respiration. This causes changes in plant and canopy reflectance, which may serve as indicators of gas leakage. In this study, a covariance analysis was performed between reflectance indices of maize (*Zea mays*) and wheat (*Triticum aestivum*) canopies and oxygen concentrations in a simulated natural gas leak. Twenty-nine days after oxygen shortage occurred, the reflectance indices had the highest correlation with oxygen concentrations in the soil, for both species. The effect was consistent within species but the absolute values varied between the species. Normalization by adding a constant value to the control index of one species resulted in significant linear regression models for several indices. The indices with the highest regression coefficients were used to predict the oxygen concentration in the soil. This showed that the gas leakage caused reflectance changes up to 0.5 m from the source. As it could not be proven that oxygen shortage was the cause of the reflectance changes, further work is needed to study the side-effects of gas leakage, such as bacterial oxygen depletion, on plant growth and reflectance.

1. Introduction

Gas pipelines that are buried in the soil leak for several reasons, of which ageing and accidents are the most common. If these leaks are large or remain undiscovered for a long time, large quantities of explosive gases can collect in the soil, giving rise to potentially dangerous situations. In the USA alone, the National Transportation Safety Board (NTSB) has reported millions of dollars in losses and several casualties due to gas pipeline leakage (NTSB 2001, 2003). The existing techniques for monitoring gas leakage are time-consuming and expensive (Tedesco 1995, Zirnig *et al.* 2002), and remote sensing has been suggested as an alternative method for leak detection (Zirnig *et al.* 2002, Van Persie *et al.* 2004). Above-ground changes in vegetation growth due to gas leakage are visible as changes in reflectance, which could serve as an indicator of gas leakage. Natural gas in the soil displaces the normal soil air, leading to a reduction in soil oxygen concentration (Hoeks 1972,

*Corresponding author. Email: marleen.noomen@tno.nl

International Journal of Remote Sensing
ISSN 0143-1161 print/ISSN 1366-5901 online
http://www.tandf.co.uk/journals
DOI: 10.1080/01431160801961383

Arthur *et al.* 1985), and consumption of methane by aerobic bacteria may further deplete soil oxygen (Steven *et al.* 2006). In general, soil oxygen shortage affects plant growth negatively, leading to reduced root and shoot growth and reduced dry weight (Drew 1991). Pysek and Pysek (1989) found that natural gas leakage decreased canopy cover, reduced species diversity, increased reflectance at red wavelengths and decreased reflectance in the near-infrared. Smith *et al.* (2004b) found a decrease in bean and wheat growth as a result of simulated gas leakage, and a change in reflectance properties in the 700–740 nm region (the 'red edge'). In another study, Smith *et al.* (2004a) demonstrated that soil oxygen displacement by natural gas, argon, nitrogen and waterlogging caused an increase in reflectance in the visible and a change in the shape and position of the red edge. These results indicated that the changes in reflectance due to gas leakage may be caused by oxygen shortage and not by the natural gas itself (Smith *et al.* 2004a). Bammel and Birnie (1994) found that the red edge was shifted towards shorter wavelengths in sagebrush as a result of hydrocarbon-induced stress, while Crawford (1986) detected an increase in reflectance in the visible light and shift in the red edge position (REP) towards shorter wavelengths in Douglas-fir trees growing in an area of hydrocarbon microseepage. By contrast, Yang *et al.* (1999) found a shift of the REP towards longer wavelengths in a wheat field located in a hydrocarbon microseepage area.

To test whether changes in soil oxygen concentrations can be related to canopy reflectance, we designed an experiment in which maize (*Zea mays*) and wheat (*Triticum aestivum*) were grown over a simulated natural gas leak. Several hyperspectral reflectance indices were calculated to study their relationship with the soil oxygen concentration. Our focus was on finding indices that can predict oxygen concentrations based on both the maize and wheat canopy reflectance and at several moments in time, increasing the probability of finding a general reflectance index that can serve as a non-destructive method for gas leak detection.

2. Methods

2.1 *Experiment set-up*

Natural gas was delivered to 2.5 m square canopy plots of maize (*Zea mays* cv *Nescio*) and wheat (*Triticum aestivum* cv *Pasteur*), located at the Sutton Bonington campus of the University of Nottingham, UK (52.8° N, 1.2° W). Two maize plots (Mg1 and Mg2) and two wheat plots (Wg1 and Wg2) received gas, while two other plots were gas free (Mc and Wc). The seeds were sown on 10 June 2003. When both species had developed four leaves and the canopy cover was at least 15%, the gas was switched on (t_1). The soil consisted of a 30 cm top layer of clay loam overlying a 70+ cm clay and marl horizon (Reeve 1975). Mains gas is dehydrated during processing (Kennedy 1993), so to avoid dehydration of the soil, the plots were watered regularly and a moist soil condition was maintained.

2.2 *Gas delivery*

Mains natural gas was delivered through a 25 mm pipe into the soil 1 m below the centre of each plot for 45 days. The gas flow, which was fixed at approximately $100\,l\,h^{-1}$, was distributed through small holes at 3 cm intervals around the lower 20 cm of the pipes. To enable soil gas and oxygen concentration measurements, four plastic tubes of 4 cm diameter were inserted in the soil up to 50 cm deep, at 50, 100, 150 and 200 cm from the edge of each plot (figure 1). A GMI Gasurveyor methane

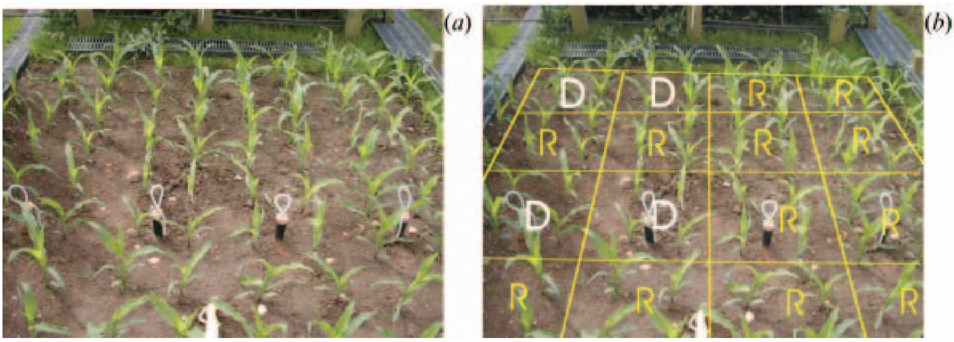

Figure 1. (*a*) Maize plot with four plastic tubes for measuring the gas concentration. (*b*) Division of the plot in virtual blocks of 50 by 50 cm. R, blocks used for reflectance measurements; D, blocks used for destructive measurements.

monitor was attached to the outflow side of each tube to measure the volume percentage of soil methane and oxygen in the soil. Gas measurements were performed daily between 0800 and 0900 h.

2.3 *Canopy growth*

On each sampling day, the average height of 12 plants per plot was measured using a stratified random sampling design (Webster and Oliver 1990). The percentage canopy cover was estimated on 50 by 50 cm squares. At t_{16} and t_{35}, leaf moisture content was measured on eight leaves from each plot centre. The leaves were clipped, weighed, cooled in ice and transported to the laboratory within 2 h after clipping. The leaves were dried in an oven at 70°C for 4 days, then weighed again, and the moisture content (MC) calculated as:

$$\mathrm{MC} = 100\frac{F-D}{F} \tag{1}$$

where F is the fresh weight and D the dry weight.

Leaf chlorophyll was measured at 29, 35 and 42 days (t_{29}, t_{35} and t_{42}) after gassing started. Four leaves were taken from each plot centre, after which chlorophyll was measured following the method described by Bruinsma (1963).

2.4 *Canopy spectral measurements*

As only three plots were available per species, the plots were divided into 16 virtual blocks of 50 by 50 cm to increase the number of observations. Twelve blocks were used for the canopy spectral measurements, while four were used for destructive analysis (respectively *R* and *D* in figure 1(*b*)). The outer 25 cm of the plots was not used for measurements to avoid edge effects. Spectral measurements were taken weekly using an ASD Fieldspec Pro spectroradiometer, which has a sampling interval between 1.4 nm and 12 nm but produces 1 nm interval readings over the full wavelength range (350–2500 nm). The sensor, a 1.5-m-long fibre optic cable with 25° field of view, was held approximately 1 m above the plant surface to view a block of 50 by 50 cm. Spectral measurements were made between 1030 and 1300 h in sunny weather. Every 10 minutes, reference measurements were taken of a halon white panel for the internal calibration of the instrument. Each spectrum is an average of 25 samples, while five spectra of each block were averaged to compensate for differences in reflectance owing to varying leaf angles (or bidirectional reflectance distribution function (BRDF)) (Nicodemus 1977, Sandmeier and Deering 1999).

2.5 *Data analysis*

It was expected that changes in oxygen concentration would affect vegetation vigour, which in turn would alter canopy reflectance. Even though this meant that there would only be an indirect relationship between oxygen concentration and reflectance, they were correlated to study the nature of their relationship. At 10 sample points (located at 25, 75 and 400 cm from the source) both the oxygen concentration and reflectance were measured. These points were used for an analysis of covariance between reflectance indices and oxygen concentration. This analysis tests whether the effect of the continuous predictor (the reflectance index) on the dependent variable (oxygen concentration) is similar for both covariates (maize and wheat). When the effect was similar, a simple linear regression analysis was used to calculate the prediction power. This was done for five time-steps (t_{16}, t_{22}, t_{29}, t_{35} and t_{42}). Fifty-one hyperspectral indices that are known to react on changes in vegetation vigour were selected for the analysis. Most indices are reflectance ratios in the visible and near-infrared, while a few indices are located in the shortwave infrared (table 1).

For prediction accuracy, only those models that had a coefficient of determination (R^2) of 0.5 or higher (arbitrarily chosen to reduce the number of weakly predicting indices) were selected for modelling oxygen concentrations under the four gassed plots and the two control plots. Based on the measured gas concentrations and the canopy patterns, the expectation was that the predicted oxygen concentration would be lowest close to the gas source, increasing with distance from the source to a value of 20% on the control plots.

3. Results

3.1 *Gas distribution*

The total amount of delivered gas varied between the different plots (table 2). However, the gas distribution within the plots was similar for each plot, with a high gas concentration in the centre of the plot and decreasing concentrations towards the edges. The oxygen concentration in the control plots was on average 20%. In the gassed plots oxygen concentrations decreased towards the centre to an average of 11% (table 2). The correlation between the gas and oxygen concentration in the soil was linear (figure 2).

3.2 *Canopy growth*

In the central 50 cm of the gassed maize plots, the average plant height was reduced by 22%, the canopy cover and number of leaves per plant by 10%, and chlorophyll content by 44% compared to the control (table 3). The height and cover of the wheat was reduced by less than 5% compared to the control, but the number of leaves in the centre 50 cm of the plot had decreased by 27% and the chlorophyll content by 50%. Outside the central 50 cm, the canopy characteristics were within 5% of the control values, except that the number of leaves of the wheat plants was reduced by 21%. Leaf moisture content was similar for the gassed and control plants at both t_{16} and t_{35} (table 3).

3.3 *Reflectance*

Commonly used reflectance indices indicated that the plants on the gassed plots were stressed: the Normalized Difference Vegetation Index (NDVI) was lower during the whole experiment, while the REP was located at shorter wavelengths (figure 3; for equations of NDVI and REP see table 1). This is in accordance with results from a study by Smith *et al.* (2004*b*), who found the REP of gassed bean and barley located at shorter wavelengths compared to control plants.

3.4 *Regression results*

A covariance analysis between each reflectance index and oxygen concentration was performed at t_{16}, t_{22}, t_{29}, t_{35} and t_{42}. Those indices that yielded significant correlations ($p<0.05$) were selected to check whether there was a difference between the maize and wheat (covariates). Nine indices resulted in significant models at t_{16}, 34 indices at t_{22}, 48 indices at t_{29} and no indices at t_{35} and t_{42}. Of these indices, two, 18 and one indices, respectively, at t_{16}, t_{22} and t_{29} predicted the oxygen concentration without species effect ('O' in table 4). Scatterplots of the indices against the oxygen concentration indicated that, although there is a difference in absolute index values, the slope of the regression equation between oxygen and index was very similar for both species (figure 4). If the difference between the absolute index values could be removed, the models would be expected to be significant without a difference between species. A simple way to remove the difference between species was to subtract the control values of wheat (Wc) from the control values of maize (Mc), and subsequently add this index difference (I_D) to all wheat values:

Step 1:

$$I_{(Mc)} - I_{(Wc)} = I_D \tag{2}$$

where $I_{(Mc)}$ is the index value of the maize control plot and $I_{(Wc)}$ is the index value of the wheat control plot;

Step 2:

$$I_{(Wg,\ Wc)} + I_D = I' \tag{3}$$

where $I_{(Wg,\ Wc)}$ is the index value at the gassed and control wheat plots, respectively. I' is then the normalized index on the wheat plots, which can be compared directly with the index values on the maize plots.

Consequently, a new covariance analysis was performed on the transformed data, which resulted in respectively 15, 20 and 20 significant models at t_{16}, t_{22}, and t_{29} in which the species effect was removed (table 4), while at t_{35} and t_{42} normalization had no effect. Besides the large increase in the number of indices that predict the oxygen concentration, normalization also resulted in a small increase in R^2 for the majority of the indices that were significantly correlated to oxygen before normalization.

Before normalization there were no indices that could predict soil oxygen at each date, yet after normalization there were six indices that could be used to predict soil oxygen at t_{16}, t_{22}, and t_{29}: CTR2, LIC1, LIC3, mNDVI705, OSAVI and NDVI705 (table 4). The highest regression coefficients were found at t_{29}.

Table 1. Reflectance indices tested in this study.

Index name	Equation	Reference
Anthocyanin Reflectance Index 1 (ARI1)	$(1/R_{550})-(1/R_{700})$	Gitelson *et al.* 2001
Anthocyanin Reflectance Index 2 (ARI2)	$R_{800}[(1/R_{550})-(1/R_{700})]$	Gitelson *et al.* 2001
Blue/Green Index (BGI1)	R_{400}/R_{550}	Zarco-Tejada *et al.* 2005
Blue/Green Index (BGI2)	R_{450}/R_{550}	Zarco-Tejada *et al.* 2005
Blue/Red Index (BRI1)	R_{400}/R_{690}	Zarco-Tejada *et al.* 2005
Blue/Red Index (BRI2)	R_{450}/R_{690}	Zarco-Tejada *et al.* 2005
Carotenoid Reflectance Index 1 (CRI1)	$(1/R_{510})-(1/R_{550})$	Gitelson *et al.* 2002
Carotenoid Reflectance Index 2 (CRI2)	$(1/R_{510})-(1/R_{700})$	Gitelson *et al.* 2002
Carter Indices (CTR)	$\mathrm{CTR1}=R_{695}/R_{420}$	Carter 1994
	$\mathrm{CTR2}=R_{695}/R_{760}$	Carter 1994
Curvature Index (CUR)	$(R_{675}R_{690})/(R_{683})^2$	Zarco-Tejada *et al.* 2000
Enhanced Vegetation Index (EVI)	$2.5(R_{\mathrm{NIR}}-R_{\mathrm{Red}})/(R_{\mathrm{NIR}}+6R_{\mathrm{Red}}-7.5R_{\mathrm{Blue}}+1)$	Huete *et al.* 1997
Gitelson and Merzlyak (GM)	$\mathrm{GM1}=R_{750}/R_{550}$	Gitelson and Merzlyak 1997
	$\mathrm{GM2}=R_{750}/R_{700}$	Gitelson and Merzlyak 1997
Improved SAVI with self-adjustment factor L (MSAVI)	$0.5\{2R_{800}+1-[(2R_{800}+1)^2-8(R_{800}-R_{670})]^{0.5}\}$	Qi *et al.* 1994
Lichtenthaler Indices (LIC)	$\mathrm{LIC1}=(R_{800}-R_{680})/(R_{800}+R_{680})$	Lichtenhaler *et al.* 1996
	$\mathrm{LIC2}=R_{440}/R_{690}$	Lichtenhaler *et al.* 1996
	$\mathrm{LIC3}=R_{440}/R_{740}$	Lichtenhaler *et al.* 1996
Modified C_{ab} Absorption in Reflectance Index (MCARI)	$[(R_{700}-R_{670})-0.2(R_{700}-R_{550})](R_{700}/R_{670})$	Daughtry *et al.* 2000
Modified Chlorophyll Absorption in Reflectance Index (MCARI1)	$1.2[2.5(R_{800}-R_{670})-1.3(R_{800}-R_{550})]$	Haboudane *et al.* 2004
Modified Chlorophyll Absorption in Reflectance Index (MCARI2)	$\frac{1.5[2.5(R_{800}-R_{670})-1.3(R_{800}-R_{550})]}{\sqrt{[(2R_{800}+1)^2-(6R_{800}-5\sqrt{R_{670}})]-0.5}}$	Haboudane *et al.* 2004
Modified Red Edge Normalized Difference Vegetation Index (mNDVI705)	$(R_{750}-R_{705})/(R_{750}+R_{705}-2R_{445})$	Sims and Gamon 2002
Modified Red Edge Simple Ratio Index (mSR705)	$(R_{750}-R_{445})/(R_{705}-R_{445})$	Sims and Gamon 2002
Modified Simple Ratio (MSR)	$(R_{\mathrm{NIR}}/R_{\mathrm{Red}}-1)/[(R_{\mathrm{NIR}}/R_{\mathrm{Red}})^{0.5}+1]$	Chen 1996
Modified Triangular Vegetation Index (MTVI1)	$1.2[1.2(R_{800}-R_{550})-2.5(R_{670}-R_{550})]$	Haboudane *et al.* 2004
Modified Triangular Vegetation Index (MTVI2)	$\frac{1.5[1.2(R_{800}-R_{550})-2.5(R_{670}-R_{550})]}{\sqrt{[(2R_{800}+1)^2-(6R_{800}-5\sqrt{R_{670}})]-0.5}}$	Haboudane *et al.* 2004
Moisture Stress Index (MSI)	R_{1599}/R_{819}	Hunt and Rock 1989

Table 1. (*Continued.*)

Index name	Equation	Reference
Normalized Difference Infrared Index (NDII)	$(R_{819}-R_{1649})/(R_{819}+R_{1649})$	Hardisky *et al.* 1983
Normalized Difference Nitrogen Index (NDNI)	$\frac{\log(1/R_{1510})-\log(1/R_{1680})}{\log(1/R_{1510})+\log(1/R_{1680})}$	Serrano *et al.* 2002
Normalized Difference Vegetation Index (NDVI)	$(R_{NIR}-R_{Red})/(R_{NIR}+R_{Red})$	Rouse *et al.* 1974
Normalized Difference Water Index (NDWI)	$(R_{857}-R_{1241})/(R_{857}+R_{1241})$	Gao 1995
Normalized Phaeophytinization Index (NPI)	$(R_{415}-R_{435})/(R_{415}+R_{435})$	Barnes 1992
Normalized Pigment Chlorophyll Index (NPCI)	$(R_{680}-R_{430})/(R_{680}+R_{430})$	Penuelas *et al.* 1994
Optimized Soil-Adjusted Vegetation Index (OSAVI)	$(1+0.16)(R_{800}-R_{670})/(R_{800}+R_{670}+0.16)$	Rondeaux *et al.* 1996
Photochemical Reflectance Index (PRI)	$(R_{531}-R_{570})/(R_{531}+R_{570})$	Gamon *et al.* 1992
Plant Senescence Reflectance Index (PSRI)	$(R_{680}-R_{500})/R_{750}$	Merzlyak *et al.* 1999
Red Edge Normalized Difference Vegetation Index (NDVI705)	$(R_{750}-R_{705})/(R_{750}+R_{705})$	Sims and Gamon 2002
Red Edge Position Index (REP)	Max. in first derivative between R_{690} and R_{740}	Curran *et al.* 1995
Red/Green Index (RGI)	R_{690}/R_{550}	Zarco-Tejada *et al.* 2005
Renormalized Difference Vegetation Index (RDVI)	$(R_{800}-R_{670})/\sqrt{(R_{800}-R_{670})}$	Rougean and Breon 1995
Simple Ratio Index (SR)	R_{NIR}/R_{Red}	Rouse *et al.* 1974
Simple Ratio Pigment Index (SRPI)	R_{430}/R_{680}	Penuelas *et al.* 1995
Structure Insensitive Pigment Index (SIPI)	$(R_{800}-R_{450})/(R_{800}+R_{650})$	Penuelas *et al.* 1995
Sum Green Index (SG)	Average of R_{500} till R_{600}	Gamon and Surfus 1999
Transformed CARI (TCARI)	$3[(R_{700}-R_{670})-0.2(R_{700}-R_{550})(R_{700}/R_{670})]$	Haboudane *et al.* 2002
Triangular Vegetation Index (TVI)	$0.5[120(R_{750}-R_{550})-200(R_{670}-R_{550})]$	Broge and Leblanc 2000
Vogelmann Indices (VOG)	$VOG1=R_{740}/R_{720}$	Vogelmann *et al.* 1993
	$VOG2=(R_{734}-R_{747})/(R_{715}+R_{726})$	Vogelmann *et al.* 1993
	$VOG3=(R_{734}-R_{747})/(R_{715}+R_{720})$	Vogelmann *et al.* 1993
Water Band Index (WBI)	R_{900}/R_{970}	Penuelas *et al.* 1997
Zarco and Miller (ZM)	R_{750}/R_{710}	Zarco-Tejada *et al.* 2001

Table 2. Average gas flow per hour under the four plots, and the average measured gas and O_2 concentrations and their standard deviations (SD) at 25 cm and 75 cm distance from the source.

Plot	Average gas flow ($l\,h^{-1}$)	Gas concentration (%) ±SD		O_2 concentration (%) ±SD	
		25 cm	75 cm	25 cm	75 cm
Maize plot 1 (Mg1)	102	10.01±7.78	1.39±1.82	12.62±4.28	17.08±1.19
Maize plot 2 (Mg2)	32	3.80±4.79	1.07±1.37	13.02±3.40	18.99±0.55
Wheat plot 1 (Wg1)	153	12.64±7.79	0.65±0.70	9.73±4.98	18.13±1.26
Wheat plot 2 (Wg2)	88	10.06±8.37	1.09±1.59	11.80±4.92	19.20±0.52
Average	93.75	9.13±7.18	1.05±1.37	11.79±4.39	18.35±0.88

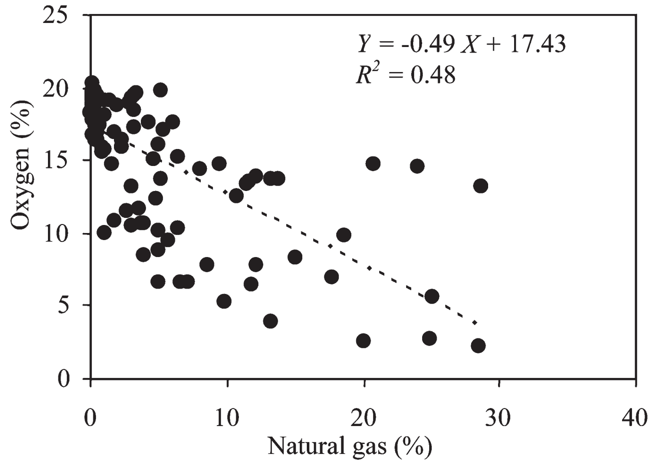

Figure 2. Measured oxygen as a function of measured natural gas concentration. The regression equation and R^2 are shown.

3.5 *Prediction of oxygen concentrations*

Overall, the regression coefficients were highest at t_{29} and lowest at t_{16}. As the analysis was based on just 10 points, an additional assessment was made of the variation of the predicted oxygen concentrations on the control plots, where

Table 3. Average canopy characteristics ± standard deviation between t_{16} and t_{42}.

Distance to source (cm)	Plant height (cm)	Canopy cover (%)	Number of leaves	Total chlorophyll ($mg\,g^{-1}$)	Leaf moisture* (%)
Maize					
0–60	80.0±23.0	67.2±17.0	8.3±1.2	1.77±0.2	83.0±0.6
61–125	97.7±11.6	75.1±1.0	9.2±0.6	3.38±0.2	–
⩾126	102.2±3.2	75.2±0.3	9.5±0.4	3.17±0.4	83.3±1.3
Wheat					
0–60	47.2±4.0	40.3±13.8	4.4±0.8	2.03±0.3	74.8±2.1
61–125	47.5±3.8	46.9±0.6	4.7±0.6	4.03±0.2	–
⩾126	48.0±2.2	42.5±1.8	6.0±1.0	4.03±0.3	74.3±1.6

*Leaf moisture was not measured in the region between 61 and 125 cm.

the oxygen concentration was 20%. The predicted control values at t_{29} were centred mostly around 20% (table 5).

Graphs of the predicted oxygen concentrations on the gassed and control plots against distance from the gas source show that, although the prediction equation was based on both species, there is a difference in prediction accuracy between the maize and wheat plots. In general, the indices performed better on the maize plots than on the wheat plots. At t_{29} the pattern of low oxygen close to the gas source, which increases with distance, was most clear on plot Mg1 (figure 5). All indices on this plot showed the same pattern. Mg2, which received less than half the amount of gas compared to Mg1, showed the same pattern when OSAVI was used but the other indices showed a less clear pattern. On both wheat plots, OSAVI was the best predictor.

For the detection of gas leaks, it is important that areas with low oxygen are clearly distinguishable from unaffected areas. An index that minimizes the differences in the control canopy, and enhances the differences between the control and the gassed canopy, is therefore preferable. Although LIC3 had the highest regression coefficient, the oxygen predicted using the control wheat plots ranged from 13% to 25%, compared to a range of 16–24% based on OSAVI. OSAVI was deemed the best predictor at t_{29} as it maximized the differences between gassed and control canopy (figure 5), while the average predicted oxygen values under the control plots were closest to 20%.

At t_{22} the indices had regression coefficients below 0.7, resulting in less reliable predictions of oxygen under the plots than at t_{29}. As at t_{29}, LIC3 for t_{22} had the highest regression coefficient, but did not predict oxygen reliably under the wheat plots. The best predictor at t_{22} was CTR2 (figure 6), although the patterns for oxygen with distance from the source were less clear than at t_{29}.

3.6 *Maximum range of affected area*

To determine the maximum distance between the gas source and the point beyond which the gas had no influence, a curve was fitted through the predicted oxygen values. To find the best-fitting curve, an assumption was made that the oxygen concentration was 0% in the centre of the gas source, and increased towards 20% at the unaffected areas. The measured oxygen concentrations O_2 in the soil followed an exponential relationship with distance:

$$O_2 = 20.0\left[1 - \exp^{(-0.033 \times D)}\right] \quad (4)$$

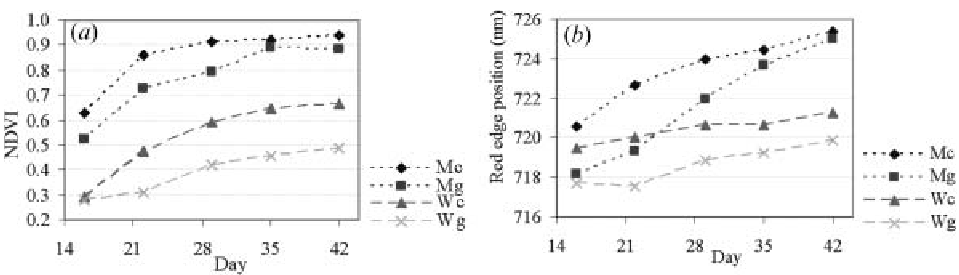

Figure 3. Variation in (*a*) Normalized Difference Vegetation Index (NDVI) and (*b*) red edge position (REP) with time. Both indices are lower on the gassed plots, suggesting that the gassed canopy is stressed.

Table 4. Significant models ($p<0.05$) and values of R^2 at three time-steps before and after normalization.

Index name	t_{16} Before		t_{16} After		t_{22} Before		t_{22} After		t_{29} Before		t_{29} After	
Anthocyanin Reflectance Index 1 (ARI1)												
Anthocyanin Reflectance Index 2 (ARI2)												
Blue/Green Index (BGI1)					OS		O	0.37	OS			
Blue/Green Index (BGI2)									OS		O	0.40
Blue/Red Index (BRI1)												
Blue/Red Index (BRI2)									OS		O	0.62
Carotenoid Reflectance Index 1 (CRI1)												
Carotenoid Reflectance Index 2 (CRI2)												
Carter Indices (CTR1)												
Carter Indices (CTR2)	O	0.47	O	0.41	OS		O	0.67	OS		O	0.82
Curvature Index (CUR)									OS			
Enhanced Vegetation Index (EVI)	OS		O	0.46	O	0.44			OS			
Gitelson and Merzlyak (GM1)			O	0.43	O	0.59	O	0.57	OS			
Gitelson and Merzlyak (GM2)					OS				OS			
Improved SAVI with self-adjustment factor L (MSAVI)	OS		O	0.51					OS			
Lichtenthaler Indices (LIC1)			O	0.33	O	0.54	O	0.62	OS		O	0.84
Lichtenthaler Indices (LIC2)									O	0.53	O	0.61
Lichtenthaler Indices (LIC3)	O	0.43	O	0.44	OS		O	0.69	OS		O	0.84
Modified C_{ab} Absorption in Reflectance Index (MCARI)	OS											
Modified Chlorophyll Absorption in Reflectance Index (MCARI1)	OS											
Modified Chlorophyll Absorption in Reflectance Index (MCARI2)	OS		O	0.45	O	0.43			OS			
Modified Red Edge Normalized Difference Vegetation Index (mNDVI705)			O	0.42	OS		O	0.67	OS		O	0.73
Modified Red Edge Simple Ratio Index (mSR705)			O	0.39	OS		O	0.60	OS			
Modified Simple Ratio (MSR)					O	0.47			OS		O	0.40
Modified Triangular Vegetation Index (MTVI1)	OS						O	0.27				
Modified Triangular Vegetation Index (MTVI2)	OS		O	0.45	O	0.37			OS			
Moisture Stress Index (MSI)					O	0.43			OS		O	0.82

Table 4. (*Continued.*)

	t_{16}			t_{22}				t_{29}		
Index name	Before	After		Before		After		Before	After	
Normalized Difference Infrared Index (NDII)								OS	O	0.76
Normalized Difference Nitrogen Index (NDNI)										
Normalized Difference Vegetation Index (NDVI)		OS		O	0.54	O	0.62	OS	O	0.84
Normalized Difference Water Index (NDWI)								OS	O	0.78
Normalized Phaeophytinization Index (NPI)				O	0.50					
Normalized Pigment Chlorophyll Index (NPCI)								OS	O	0.70
Optimized Soil-Adjusted Vegetation Index (OSAVI)	OS	O	0.43	O	0.55	O	0.53	OS	O	0.64
Photochemical Reflectance Index (PRI)				O	0.47	O	0.54	OS	O	0.58
Plant Senescence Reflectance Index (PSRI)				O	0.52	O	0.56	OS		
Red Edge Normalized Difference Vegetation Index (NDVI705)		O	0.42	OS		O	0.67	OS	O	0.72
Red Edge Position Index (REP)				O	0.60	O	0.64	OS		
Red/Green Index (RGI)								OS	O	0.78
Renormalized Difference Vegetation Index (RDVI)	OS	O	0.51	O	0.48			OS		
Simple Ratio Index (SR)										
Simple Ratio Pigment Index (SRPI)								OS	O	0.66
Structure Insensitive Pigment Index (SIPI)		OS	0.32	O	0.57	O	0.59	OS	O	0.77
Sum Green Index (SG)										
Transformed CARI (TCARI)	OS									
Triangular Vegetation Index (TVI)	OS									
Vogelmann Indices (VOG1)		O	0.40	O	0.56	O	0.63	OS		
Vogelmann Indices (VOG2)				O	0.58	O	0.61	OS		
Vogelmann Indices (VOG3)				O	0.57	O	0.60	OS		
Water Band Index (WBI)				OS		O	0.53	OS	O	0.75
Zarco and Miller (ZM)		O	0.42	OS		O	0.59	OS		

OS, significant for oxygen and species, that is there is a significant difference between maize and wheat; O, significant for oxygen only.

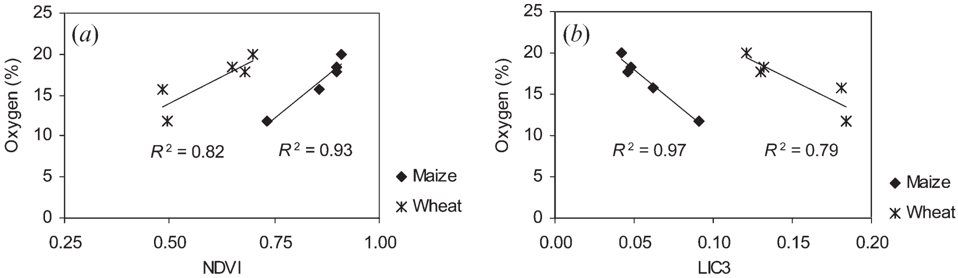

Figure 4. Covariance analysis shows that a regression between (*a*) NDVI and (*b*) LIC3 against oxygen concentration results in similar slopes but different intercepts for the two species.

Table 5. Predicted oxygen concentrations ± standard error under the control maize and wheat plots (n=24) at three time-steps.

Index	t_{16}	t_{22}	t_{29}
LIC1	17.61 ± 1.23	19.17 ± 1.75	19.39 ± 2.40
LIC3	18.01 ± 1.78	18.84 ± 1.73	19.52 ± 2.38
CTR2	18.08 ± 1.42	19.13 ± 2.48	19.32 ± 2.65
mNDVI705	18.50 ± 1.39	20.12 ± 1.70	19.23 ± 2.23
NDVI705	18.46 ± 1.42	20.28 ± 2.13	19.30 ± 2.00
OSAVI	18.02 ± 1.51	17.95 ± 0.66	20.12 ± 1.84
Mean	18.11 ± 1.46	19.25 ± 1.74	19.48 ± 2.25

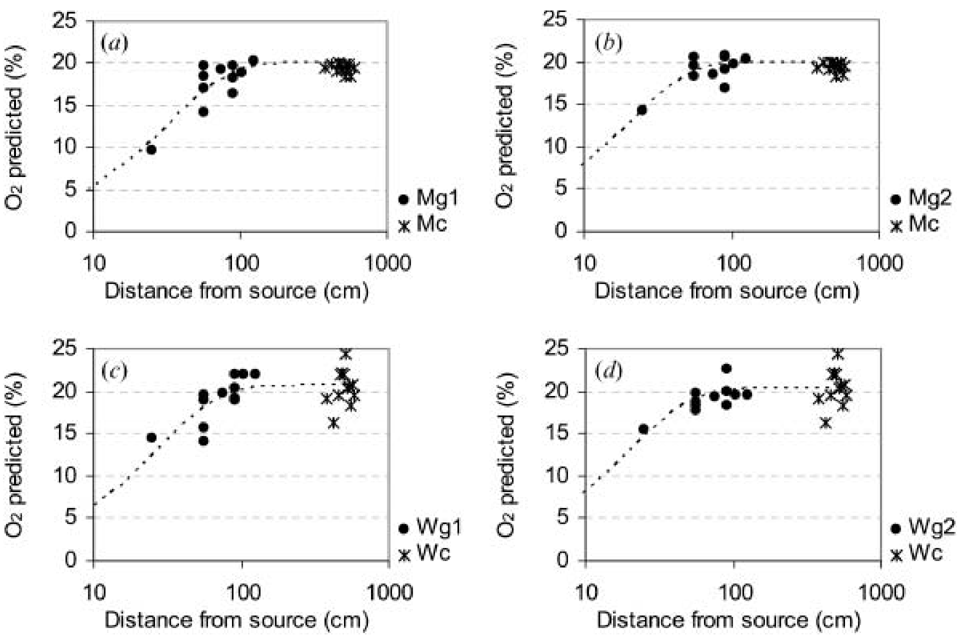

Figure 5. Predicted oxygen concentrations of (*a*) Mg1 and Mc, (*b*) Mg2 and Mc, (*c*) Wg1 and Wc, and (*d*) Wg2 and Wc at t_{29}, based on OSAVI. An exponential curve that describes the oxygen pattern is fitted to the data.

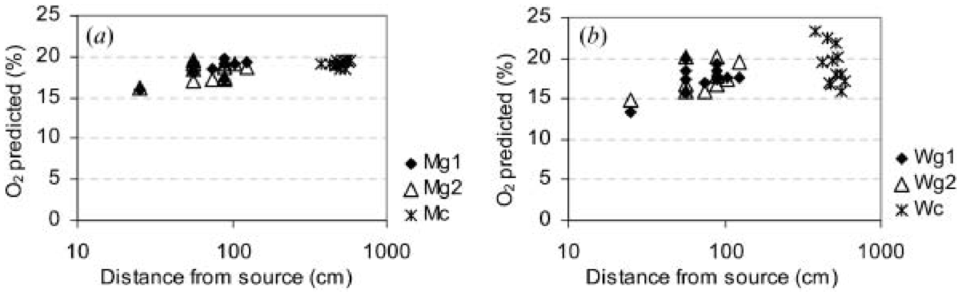

Figure 6. Predicted oxygen concentrations of (*a*) Mg1, Mg2, Mc and (*b*) Wg1, Wg2, Wc at t_{22} based on CTR2.

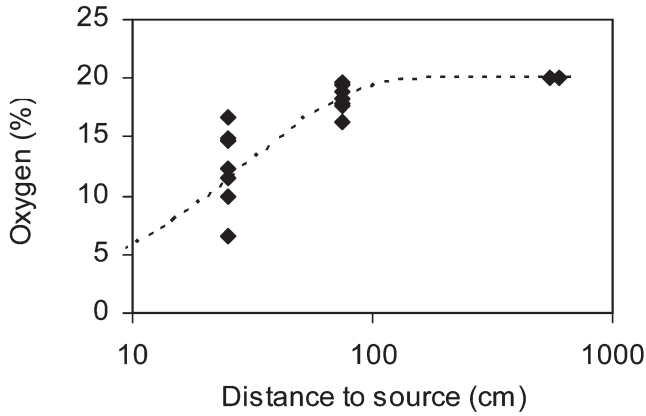

Figure 7. Measured oxygen concentrations on all analysed plots with exponential fit (R^2 of 0.94)

where 20.0 is the maximum oxygen concentration, −0.033 defines the shape of the fitted curve, and D is the distance to the gas source (R^2 0.94; figure 7).

The same distribution was found in the predicted oxygen values. An exponential curve was fitted through the predicted oxygen values on each plot and subsequently the distance was determined beyond which the oxygen concentrations were not distinguishable from those of the control. As the control concentrations contained minimum values of 18.2% (t_{29}) and 16.6% (t_{22}), only values lower than these are likely to be caused by gas in the soil. Therefore, the distance was calculated from the gas source to the point where the oxygen concentration was 16% (table 6). The distances beyond which the oxygen values were not distinguishable from the control ranged from 30 to 50 cm, depending on the amount of gas the plot received and on the species.

Table 6. Distance from gas source to point where the oxygen concentration is 16% at t_{29}.

Plot	Distance (cm)
Mg1	51.5
Mg2	31.9
Wg1	40.0
Wg2	30.5

4. Discussion

In this study, maize and wheat plant growth had a comparable reaction to gas in the soil: only the plants growing within 50 cm of the gas source (where the average oxygen concentration was 11%) were severely stunted. There are several possible reasons for the changes in plant growth. One is that the measured oxygen concentrations in the gassed plots were well below ambient soil oxygen concentrations. In general, oxygen deficiency disturbs metabolic processes in the plant, resulting in reduced growth (Drew 1991), although rice (*Oryza sativa*) is a well-known exception (Jackson and Pearce 1991, Justin and Armstrong 1991). The reaction of plants to soil oxygen shortage depends on the duration of the oxygen shortage and the species, as well as on the cultivar (Huang *et al.* 1994, 1997, Zaidi *et al.* 2003), and conflicting results are reported about the concentrations at which O_2 becomes limiting to plant growth (Armstrong 1979).

In addition to the direct effect of reduced oxygen concentrations on plant growth, oxygen shortage caused by gas leakage may cause changes in the redox potential and the pH, leading to changes in mineralogy and nutrient availability (Schumacher 1996).

Another reason for the reduced plant growth could be the effect of natural gas itself. However, previous studies have suggested that methane is harmless to plant roots (Arthur *et al.* 1985, Smith *et al.* 2004a). As the soil oxygen concentrations in this study were very low, it is assumed that any effect of methane on the roots would be insignificant compared to the effect of the oxygen shortage. Bacterial methane oxidation, during which bacterial by-products and carbon dioxide are produced (Steven *et al.* 2006), may have been of more importance to plant growth. Literature on the effects of soil CO_2 on plant growth is sparse, but both Boru *et al.* (2003) and Huang *et al.* (1997) showed that soil CO_2 concentrations ranging from 10% to 50% caused a reduction in leaf chlorophyll content for at least some of the plants tested. CO_2 concentrations in gas leaks rarely reach such high values (Steven *et al.* 2006), yet future work could include measuring CO_2 values during gas leakage to provide information about the extent of methane oxidation.

Atmospheric methane concentrations were not measured on a continuous basis in this experiment but it is assumed that the effects on plant growth were minimal. Gustafson (1944) showed that above-ground parts of plants were not affected by 2% methane in the atmosphere. Natural gas is lighter than air, so the gas can disperse quickly. We did attempt to measure methane concentrations in the atmosphere above the gassed plots but the gas dispersed too quickly to be detected.

Finally, a shortage of soil moisture due to the drying effect of the gas may have affected plant growth. The high gas flow in the gas plots could potentially dry out the soil, which could result in reduced water uptake by the plants. To avoid this, the soil was kept moist by watering the plots regularly. Leaf moisture measurements showed that the leaf water content of the gassed plants was similar to the water content of the control plants, which suggests that the gas leakage did not lead to water shortage. To control for the possible effects of decreased soil moisture, future experiments should include a control plot to which normal air is delivered in similar quantities as the natural gas.

4.1 *Regression analysis*

The indices used in this study were all based on canopy characteristics, such as canopy density and chlorophyll content, leading to a clearly visible difference between index values of the control and gassed canopies. Figure 3 shows that the indices of maize and wheat exhibited a similar pattern in time but there was a difference in absolute values between the species. In the regression analysis between measured oxygen concentrations and reflectance indices, this was visible as a similar slope for both species but a different intercept (figure 4). The main reason for the difference in absolute values is the difference in canopy cover, which was on average 75% for the maize plots and 40% for the wheat plots. Canopy cover has been shown to be linearly or logarithmically related to reflectance indices based on the visible and near-infrared light, such as the NDVI, the type of relationship being dependent on the index (Daughtry *et al.* 2000, Thenkabail *et al.* 2000). Consequently, the difference in canopy cover caused the difference in absolute values between the species.

As the focus of this paper was on finding a reflectance index that could be used to detect low oxygen concentrations due to gas leakage for different species, the absolute difference was removed using a simple normalization based on the indices of the unaffected canopy. In this experiment, there were distinct treatment and control canopies, but in reality it may be difficult to determine which is the unaffected canopy. However, when this method was applied to detect leaks in gas pipelines, the location of the pipeline would generally be known. The control canopy could then be assumed to be more than 5 m away from the pipeline, and an average value of several pixels could serve as control index for a certain species.

Normalization resulted in several indices that could predict oxygen concentrations for both species, although at t_{29} the models yielded the highest regression coefficients. At an earlier stage, the models are less powerful because of the lower canopy cover, while at a later stage regression between indices and oxygen was not possible. The reason for this is that, after t_{29}, the maize plants growing adjacent to the centre 50 cm of the gassed plots grew so large that they partly covered the gassed area, leading to false canopy reflectance indices (figure 8). Therefore, at t_{29} the probability of detecting gas leakage is highest, which is approximately halfway through the growth cycle of maize and wheat (Grubben and Soetjipto Partohardjono 1996) and 1 month after the gas was switched on. This is in accordance with the findings by Pysek and Pysek (1989), who noted the first changes in leaf reflectance on plants growing in a simulated gas leak after 15 to 30 days. Smith *et al.* (2004b) found the first visible stress symptoms in grass that was gassed with natural gas 1.5 months after the gassing started, but this experiment took place in autumn, when the metabolic activity of the roots is low and plants are less sensitive to oxygen shortage (Smith *et al.* 2004b).

Although the regression analysis was conducted between measured oxygen concentrations and hyperspectral reflectance indices, there is no evidence that the relationship is causal. As discussed earlier, the relationship between the oxygen and the reflectance is indirect. Moreover, the changes in plant growth on the gassed plots may have been caused by the oxygen shortage itself, but are more likely to be the result of a combination of factors related to the gas leakage. As many unknown factors influence the vegetation, it cannot be said with certainty that the patterns in the canopy are caused by oxygen shortage alone. Therefore, the predicted oxygen concentrations under the canopies should be considered as an indication of the presence of gas leakage.

Extrapolation of the indices to the control and gassed plots showed that although the regression equation was based on both species, in the field it performed better on the maize than on the wheat canopy. This was because the original regression fit was stronger for the maize than for the wheat, if the species were separated (figure 4). Moreover, because of the saturation of vegetation indices at high foliage cover (Rondeaux *et al.* 1996, Daughtry *et al.* 2000, Thenkabail *et al.* 2000), subtle changes in maize canopy structure caused by factors other than soil gas were less pronounced than in the low cover of the wheat canopy, where even a small change in the alignment of leaves could change the amount of soil visible to the sensor (figure 8). These properties resulted in very similar predicted oxygen values by all tested indices under the maize canopy, but in differences under the wheat canopy. At t_{29}, LIC3 had the highest regression coefficient but on the control plots it performed worse than the best predictor OSAVI. LIC3 is based on 440 and 740 nm, wavelengths that are mainly affected by leaf chlorophyll content, internal leaf structure and leaf area (Knipling 1970, Gausman 1974, Lichtenthaler *et al.* 1996). OSAVI is based on 670 and 800 nm, wavelengths that are affected by the same plant characteristics as LIC3, but OSAVI is adjusted to remove soil variability (Rondeaux *et al.* 1996). As the wheat canopy cover was only 40%, the soil had a major influence. Even though the soil type under both plots was the same, adjusting for soil variability reduced the standard deviation in oxygen predictions under the control plots by 9%, increasing the reliability of the oxygen predictions.

At t_{22} the predicted oxygen values were overall less accurate, particularly under the wheat canopy. The predicted O_2 control values ranged from 14% to 25% for LIC3, which had the highest regression coefficients but the worst prediction under the wheat canopy. Although at t_{22} the canopy cover was even lower than at t_{29}, CTR2 (based on 695 nm and 760 nm) was a better predictor than OSAVI. Daughtry *et al.* (2000) demonstrated that indices that are insensitive to soil reflectance, such as OSAVI, are mostly related to canopy characteristics, such as LAI and foliage cover, and less to chlorophyll differences. By contrast, Carter's stress index has been shown to be sensitive to changes in chlorophyll (Carter 1994, Carter and Miller 1994). At

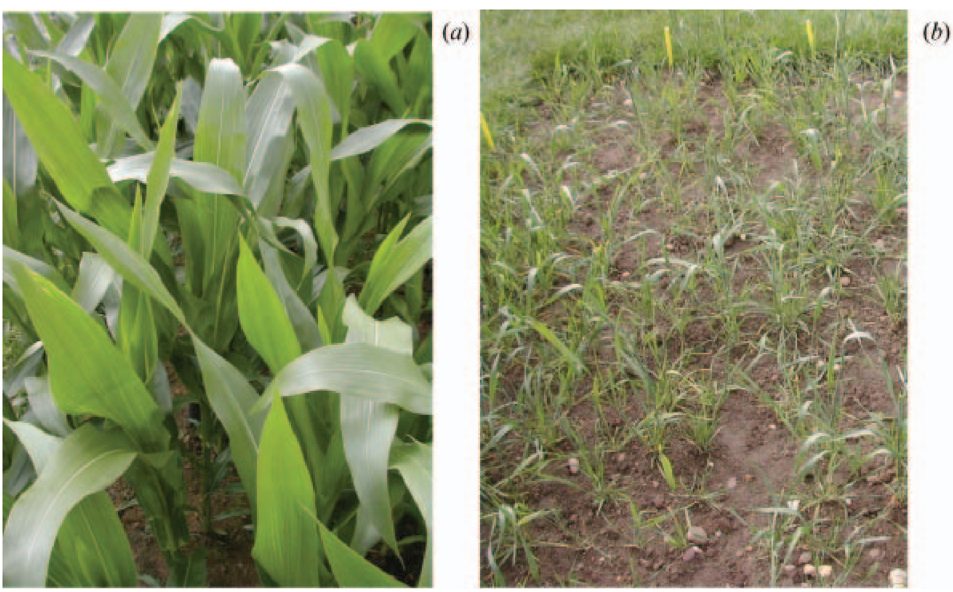

Figure 8. (*a*) Maize canopy and (*b*) wheat canopy at t_{29}.

Table 7. Regression equations for the six indices that were significant for three time-steps. O_2 is the oxygen concentration (%) in the soil. The equations at t_{16} are not shown as their regression coefficient was lower than 0.5.

t_{29}	t_{22}
$O_2=-21.19+44.47\times$ LIC1	$O_2=-1.64+24.26\times$ LIC1
$O_2=25.99-156.0\times$ LIC3	$O_2=24.97-89.80\times$ LIC3
$O_2=23.49-48.68\times$ CTR2	$O_2=22.25-25.27\times$ CTR2
$O_2=-12.13+42.37\times$ mNDVI705	$O_2=0.86+27.84\times$ mNDVI705
$O_2=-9.95+42.16\times$ NDVI705	$O_2=1.40+30.36\times$ NDVI705
$O_2=-6.74+32.10\times$ OSAVI	$O_2=1.65+22.95\times$ OSAVI

t_{22}, the differences in canopy cover between the gassed and control plots were less pronounced than at t_{29} (visible in the slope of the regression equations, table 7). Therefore, we assume that at t_{29}, the differences in canopy cover were so pronounced that differences in leaf chlorophyll were overshadowed, while at t_{22}, chlorophyll differences were relatively more pronounced because of the less dense cover. This is seen in the REP, which is in general a good predictor of chlorophyll content (Horler *et al.* 1983, Boochs *et al.* 1990): at t_{22} the difference in REP between gassed and control canopy is larger than at t_{29} (figure 3). This resulted in CTR2 being the best predictor at t_{22} and OSAVI being the best predictor at t_{29}.

The maximum distance from the gas source at which the gas leakage could be predicted in this study was 50 cm. As seen in figure 5, the lowest oxygen concentrations occurred within 50 cm, but the exponential fit shows a decrease starting approximately 100 cm from the source. As the gas leaked from a point source, low oxygen concentrations could be detected in a circle of 1 m diameter around the source, increasing the leak to a 2 m round-shaped feature. Thus, to detect gas leakage by remote sensing, the sensor should have a spatial resolution of at least 1 m. Hyperspectral sensors of this resolution do not exist at present. To increase the possibility of detecting small gas leaks, the profile of the leak could be incorporated. Incorporation of spatial information significantly improved the detection chance of natural gas seepages in Hungary and California (Van der Werff and Lucieer 2004, Van der Werff *et al.* 2006). We hypothesized that if the search for gas leaks incorporated the profile of the leak, being in the form of the exponential fit as in equation (4), this would increase the chance of leak detection. The reason for the small extent of the high gas/low oxygen area in this study was that the gas pipe was situated in the clay layer. Gas diffusion is dependent on soil porosity, soil structure (preferential pathways), and moisture content of the soil (Batjes and Bridges 1992, Moldrup *et al.* 2000). Due to the low porosity of the clay, the gas did not spread far from the exit point of the pipe. In less dense soil, the gas would probably spread further, which would enhance the chance of leakage detection.

5. Conclusions

The relationship between low soil oxygen concentrations resulting from underground gas leakage and canopy reflectance was studied. Although this relationship is not causal, several reflectance indices based on maize (*Zea mays*) and wheat (*Triticum aestivum*) canopy were linearly related to oxygen concentrations in the soil. After normalization between species, six reflectance indices could predict the soil oxygen concentrations under the canopy at three time-steps. However, the performance of each index varied with time, resulting in the best predictions 29 days after gassing started, which was halfway through the growth cycle of the plants. Due to the changing canopy characteristics, it was not possible to find one reflectance index that could be used at any time during the growth cycle. Whereas at t_{29} OSAVI was the best predictor based on the differences in canopy cover, at t_{22} CTR2 was the best predictor because of the less dense canopy and larger differences in leaf chlorophyll concentrations. Although the maximum distance at which gas leakage could be detected based on oxygen concentrations was within 50 cm of the source, the chance of detection would be increased by allowing for the exponential soil oxygen profile. As the changes in canopy reflectance have not proven to be caused by changes in oxygen alone, future work is needed on this topic to control for soil moisture changes and bacterial oxygen depletion.

Acknowledgements
We thank Matthew Beardsley for his help in the field and Dr David Rossiter for his advice on the statistical analysis. We acknowledge two anonymous reviewers for their valuable comments and suggestions.

References

ARMSTRONG, W., 1979, Aeration in higher plants. In *Advances in Botanical Research*, H.W. Woolhouse, (Ed.), pp. 226–332 (London: Academic Press).

ARTHUR, J.J., LEONE, I.A. and FLOWER, F.B., 1985, The response of tomato plants to simulated landfill gas mixtures. *Journal of Environmental Sciences and Health*, **A20**, pp. 913–925.

BAMMEL, B.H. and BIRNIE, R.W., 1994, Spectral reflectance response of big sagebrush to hydrocarbon-induced stress in the Bighorn Basin, Wyoming. *Photogrammetric Engineering and Remote Sensing*, **60**, pp. 87–96.

BARNES, J.D., 1992, A reappraisal of the use of DMSO for the extraction and determination of chlorophylls *a* and *b* in lichens and higher plants. *Environmental Experimental Botany*, **2**, pp. 85–100.

BATJES, N.H. and BRIDGES, E.M., 1992, *A Review of Soil Factors and Processes that Control Fluxes of Heat, Moisture and Greenhouse Gases* (Wageningen: ISRIC).

BOOCHS, F., KUPFER, G., DOCKTER, K. and KÜHBAUCH, W., 1990, Shape of the red edge as vitality indicator for plants. *International Journal of Remote Sensing*, **11**, pp. 1741–1753.

BORU, G., VANTOAI, T., ALVES, J., HUA, D. and KNEE, M., 2003, Responses of soybean to oxygen deficiency and elevated root-zone carbon dioxide concentration. *Annals of Botany*, **91**, pp. 447–453.

BROGE, N.H. and LEBLANC, E., 2000, Comparing prediction power and stability of broadband and hyperspectral vegetation indices for estimation of green leaf area index and canopy chlorophyll density. *Remote Sensing of Environment*, **76**, pp. 156–172.

BRUINSMA, J., 1963, The quantitative analysis of chlorophylls *a* and *b* in plant extracts. *Photochemistry and Photobiology*, **2**, pp. 241–249.

CARTER, G.A., 1994, Ratios of leaf reflectances in narrow wavebands as indicators of plant stress. *International Journal of Remote Sensing*, **15**, pp. 697–703.

CARTER, G.A. and MILLER, R.L., 1994, Early detection of plant stress by digital imaging within narrow stress-sensitive wavebands. *Remote Sensing of Environment*, **50**, pp. 295–302.

CHEN, J., 1996, Evaluation of vegetation indices and modified simple ratio for boreal applications. *Canadian Journal of Remote Sensing*, **22**, pp. 229–242.

CRAWFORD, M.F., 1986, Preliminary evaluation of remote sensing data for detection of vegetation stress related to hydrocarbon microseepage: mist gas field, Oregon. In

Proceedings of the Fifth Thematic Conference: Remote Sensing for Exploration Geology, Reno, Nevada, pp. 161–177 (Ann Arbor: Environmental Research Institute of Michigan).

CURRAN, P.J., WINDHAM, W.R. and GHOLZ, H.L., 1995, Exploring the relationship between reflectance red edge and chlorophyll concentration in slash pine leaves. *Tree Physiology*, **15**, pp. 203–206.

DAUGHTRY, C.S.T., WALTHALL, C.L., KIM, M.S., BROWN DE COLSTOUN, E. and MCMURTREY, J.E., 2000, Estimating corn leaf chlorophyll concentration from leaf and canopy reflectance. *Remote Sensing of Environment*, **74**, pp. 229–239.

DREW, M.C., 1991, Oxygen deficiency in the root environment and plant mineral nutrition. In *Plant Life under Oxygen Deprivation*, M.B. Jackson, D.D. Davies and H. Lambers (Eds), pp. 303–316 (The Hague: SPB Academic Publishing).

GAMON, J.A., PENUELAS, J. and FIELD, C.B., 1992, A narrow-waveband spectral index that tracks diurnal changes in photosynthetic efficiency. *Remote Sensing of Environment*, **41**, pp. 35–44.

GAMON, J.A. and SURFUS, J., 1999, Assessing leaf pigment content and activity with a reflectometer. *New Phytologist*, **143**, pp. 105–117.

GAO, B.C., 1995, Normalized difference water index for remote sensing of vegetation liquid water from space. *Proceedings of SPIE*, **2480**, pp. 225–236.

GAUSMAN, H.W., 1974, Leaf reflectance of near-infrared. *Photogrammetric Engineering and Remote Sensing*, **40**, pp. 183–192.

GITELSON, A.A. and MERZLYAK, M.N., 1997, Remote estimation of chlorophyll content in higher plant leaves. *International Journal of Remote Sensing*, **18**, pp. 2691–2697.

GITELSON, A.A., MERZLYAK, M.N. and CHIVKUNOVA, O.B., 2001, Optical properties and nondestructive estimation of anthocyanin content in plant leaves. *Photochemistry and Photobiology*, **71**, pp. 38–45.

GITELSON, A.A., ZUR, Y., CHIVKUNOVA, O.B. and MERZLYAK, M.N., 2002, Assessing carotenoid content in plant leaves with reflectance spectroscopy. *Photochemistry and Photobiology*, **75**, pp. 272–281.

GRUBBEN, G.J.H., and SOETJIPTO PARTOHARDJONO, F. (Eds), 1996, *PROSEA: Plant Resources of South-East Asia* (Leiden: Backhuys).

GUSTAFSON, F.G., 1944, Is natural gas injurious to flowering plants? *Plant Physiology*, **19**, pp. 551–558.

HABOUDANE, D., MILLER, J.R., PATTEY, E., ZARCO-TEJADA, P.J. and STRACHAN, I., 2004, Hyperspectral vegetation indices and novel algorithms for predicting green LAI of crop canopies: modeling and validation in the context of precision agriculture. *Remote Sensing of Environment*, **90**, pp. 337–352.

HABOUDANE, D., MILLER, J.R., TREMBLAY, N., ZARCO-TEJADA, P.J. and DEXTRAZE, L., 2002, Integrated narrow-band vegetation indices for prediction of crop chlorophyll content for application to precision agriculture. *Remote Sensing of Environment*, **81**, pp. 416–426.

HARDISKY, M.A., KLEMAS, V. and SMART, R.M., 1983, The influence of soil salinity, growth form, and leaf moisture on the spectral reflectance of *Spartina alterniflora* canopies. *Photogrammetric Engineering and Remote Sensing*, **49**, pp. 77–83.

HOEKS, J., 1972, Changes in composition of soil air near leaks in natural gas mains. *Technical Bulletin/Institute for Land and Water Management Research*, **82**, pp. 46–54.

HORLER, D.N.H., DOCKRAY, M. and BARBER, J., 1983, The red edge of plant leaf reflectance. *International Journal of Remote Sensing*, **4**, pp. 273–288.

HUANG, B., JOHNSON, J.W. and NESMITH, D.S., 1997, Responses to root-zone CO_2 enrichment and hypoxia of wheat genotypes differing in waterlogging tolerance. *Crop Science*, **37**, pp. 464–468.

HUANG, B., JOHNSON, J.W., NESMITH, D.S. and BRIDGES, D.C., 1994, Root and shoot growth of wheat genotypes in response to hypoxia and subsequent resumption of aeration. *Crop Science*, **34**, pp. 1538–1544.

Huete, A.R., Liu, H., Batchily, K. and Van Leeuwen, W., 1997, A comparison of vegetation indices over a global set of TM images for EOS-MODIS. *Remote Sensing of Environment*, **59**, pp. 440–451.

Hunt, E.R. and Rock, B.N., 1989, Detection of changes in leaf water content using near- and middle-infrared reflectances. *Remote Sensing of Environment*, **30**, pp. 43–54.

Jackson, M.B. and Pearce, D.M.E., 1991, Hormones and morphological adaptation to aeration stress in rice. In *Plant Life under Oxygen Deprivation*, M.B. Jackson, D.D. Davies and H. Lambers (Eds), pp. 47–67 (The Hague: SPB Academic Publishing).

Justin, S.H.F.W. and Armstrong, W., 1991, Evidence for the involvement of ethene in aerenchyma formation in adventitious roots of rice (*Oryza sativa* L.). *New Phytologist*, **117**, pp. 49–62.

Kennedy, J.L., 1993, *Oil and Gas Pipeline Fundamentals*, 2nd edn (Oklahoma: PennWell Publishing Company).

Knipling, E.B., 1970, Physical and physiological basis for the reflectance of visible and near-infrared radiation from vegetation. *Remote Sensing of Environment*, **1**, pp. 155–159.

Lichtenhaler, H.K., Lang, M., Sowinska, M., Heisel, F. and Mieh, J.A., 1996, Detection of vegetation stress via a new high resolution fluorescence imaging system. *Journal of Plant Physiology*, **148**, pp. 599–612.

Merzlyak, J.R., Gitelson, A.A., Chivkunova, O.B. and Rakitin, V.Y., 1999, Non-destructive optical detection of pigment changes during leaf senescence and fruit ripening. *Physiologia Plantarum*, **106**, pp. 135–141Pipelove Accident Report NTSB/PAR-00/01,

Moldrup, P., Olesen, T., Schjønning, P., Yamaguchi, T. and Rolston, D.E., 2000, Predicting the gas diffusion coefficient in undisturbed soil from soil water characteristics. *Soil Science Society of America Journal*, **64**, pp. 94–100.

Nicodemus, F.E., 1977, *Geometrical Considerations and Nomenclature for Reflectance*, National Bureau of Standards Monograph No. 160 (Washington, DC: US Department of Commerce).

NTSB, 2001, *Natural Gas Explosion and Fire in South Riding, Virginia*, Pipeline Accident Report NTSB/PAR-00/01, July 7, 1998 (Washington, DC: National Transportation Safety Board).

NTSB, 2003, *Natural Gas Pipeline Rupture and Fire Near Carlsbad, New Mexico*, Pipeline Accident Report NTSB/PAR-03/01, August 19, 2000 (Washington, DC: National Transportation Safety Board).

Penuelas, J., Filella, I., Lloret, P., Munoz, F. and Vilajeliu, M., 1995, Reflectance assessment of mite effects on apple trees. *International Journal of Remote Sensing*, **16**, pp. 2727–2733.

Penuelas, J., Gamon, J.A., Fredeen, A.L., Merino, J. and Field, C.B., 1994, Reflectance indices associated with physiological changes in nitrogen and water-limited sunflower leaves. *Remote Sensing of Environment*, **48**, pp. 135–146.

Penuelas, J., Pinol, J., Ogaya, R. and Filella, I., 1997, Estimation of plant water concentration by the reflectance water index WI (R900/R970). *International Journal of Remote Sensing*, **18**, pp. 2869–2875.

Pysek, P. and Pysek, A., 1989, Vegetation caused by experimental leakage of natural gas. *Weed Research*, **29**, pp. 193–204.

Qi, J., Chehbouni, A., Huete, A.R., Keer, Y.H. and Sorooshian, S., 1994, A modified soil vegetation adjusted index. *Remote Sensing of Environment*, **48**, pp. 119–126.

Reeve, M.J., 1975, *Soils in Derbyshire II*, Soil Survey Record, No. 27 (Dorking, Adlard and Son Ltd., Bartholomew Press).

Rondeaux, G., Steven, M. and Baret, F., 1996, Optimization of soil-adjusted vegetation indices. *Remote Sensing of Environment*, **55**, pp. 95–107.

Rougean, J.L. and Breon, F.M., 1995, Estimating PAR absorbed by vegetation from bidirectional reflectance measurements. *Remote Sensing of Environment*, **51**, pp. 375–384.

ROUSE, J.W., HAAS, R.H. and SCHELL, J.A., 1974, *Monitoring the Vernal Advancement of Retrogradiation of Natural Vegetation* (Greenbelt, MD: NASA/GSFC).

SANDMEIER, S. and DEERING, D.W., 1999, Structure analysis and classification of boreal forests using airborne hyperspectral BRDF data from ASAS. *Remote Sensing of Environment*, **69**, pp. 281–295.

SCHUMACHER, D., 1996, Hydrocarbon-induced alteration of soils and sediments. In *Hydrocarbon Migration and its Near-Surface Expression*, D. Schumacher and M.A. Abrams (Eds). AAPG Memoir 66, pp. 71–89 (Tulsa: AAPG).

SERRANO, L., PENUELAS, J. and USTIN, S.L., 2002, remote sensing of nitrogen and lignin in Mediterranean vegetation from AVIRIS data: decomposing biochemical from structural signals. *Remote Sensing of Environment*, **81**, pp. 355–364.

SIMS, D.A. and GAMON, J.A., 2002, Relationships between leaf pigment content and spectral reflectance across a wide range of species, leaf structures and developmental stages. *Remote Sensing of Environment*, **81**, pp. 337–354.

SMITH, K.L., STEVEN, M.D. and COLLS, J.J., 2004a, Spectral responses of pot-grown plants to displacement of soil oxygen. *International Journal of Remote Sensing*, **25**, pp. 4395–4410.

SMITH, K.L., STEVEN, M.D. and COLLS, J.J., 2004b, Use of hyperspectral derivative ratios in the red-edge region to identify plant stress responses to gas leaks. *Remote Sensing of Environment*, **92**, pp. 207–217.

STEVEN, M.D., SMITH, K.L., BEARDSLEY, M.D. and COLLS, J.J., 2006, Oxygen and methane depletion in soil affected by leakage of natural gas. *European Journal of Soil Science*, **57**, pp. 800–807.

TEDESCO, S.A., 1995, *Surface Geochemistry in Petroleum Exploration* (New York: Chapman & Hall).

THENKABAIL, P.S., SMITH, R.B. and DE PAUW, E., 2000, Hyperspectral vegetation indices and their relationships with agricultural crop characteristics. *Remote Sensing of Environment*, **71**, pp. 158–182.

VAN DER WERFF, H.M.A., BAKKER, W.H., VAN DER MEER, F.D. and SIDERIUS, W., 2006, Combining spectral signals and spatial patterns using multiple Hough transforms: an application for detection of natural gas seepages. *Computers and Geosciences*, **32**, pp. 1334–1343.

VAN DER WERFF, H.M.A. and LUCIEER, A., 2004, A contextual algorithm for detection of mineral alteration halos with hyperspectral remote sensing. In *Remote Sensing Image Analysis: Including the Spatial Domain*, S.M. de Jong and F.D. van der Meer (Eds), pp. 201–210 (Dordrecht, the Netherlands: Kluwer Academic Publishers).

VAN PERSIE, M., VAN DER KAMP, A. and ALGRA, T., 2004, Simulation and optimisation of a high resolution optical remote sensing system for monitoring for the European gas pipeline network. In *Proceedings of the 20th ISPRS Congress*, Istanbul, Turkey. Available online at: www.isprs.org.

VOGELMANN, J.E., ROCK, B.N. and MOSS, D.M., 1993, Red edge spectral measurements from sugar maple leaves. *International Journal of Remote Sensing*, **14**, pp. 1563–1575.

WEBSTER, R. and OLIVER, M.A., 1990, *Statistical Methods in Soil and Land Resource Survey* (New York: Oxford University Press).

YANG, H., ZHANG, J., VAN DER MEER, F. and KROONENBERG, S.B., 1999, Spectral characteristics of wheat associated with hydrocarbon microseepages. *International Journal of Remote Sensing*, **20**, pp. 807–813.

ZAIDI, P.H., RAFIQUE, S. and SINGH, N.N., 2003, Response of maize (*Zea mays* L.) genotypes to excess soil moisture stress: morpho-physiological effects and basis of tolerance. *European Journal of Agronomy*, **19**, pp. 283–399.

ZARCO-TEJADA, P.J., BERJON, A., LOPEZ-LOZANO, R., MILLER, J.R., MARTIN, P., CACHORRO, V., GONZALEZ, M.R. and DE FRUTOS, A., 2005, Assessing vineyard condition with hyperspectral indices: leaf and canopy reflectance simulation in a row-structured discontinuous canopy. *Remote Sensing of Environment*, **99**, pp. 271–287.

ZARCO-TEJADA, P.J., MILLER, J.R., MOHAMMED, G.H. and NOLAND, T.L., 2000, Chlorophyll fluorescence effects on vegetation apparent reflectance. I. Leaf level measurements and simulation of reflectance and transmittance spectra. *Remote Sensing of Environment*, **74**, pp. 582–595.

ZARCO-TEJADA, P.J., MILLER, J.R., MOHAMMED, G.H., NOLAND, T.L. and SAMPSON, P.H., 2001, Scaling-up and model inversion methods with narrow-band optical indices for chlorophyll content estimation in closed forest canopies with hyperspectral data. *IEEE Transactions on Geoscience and Remote Sensing*, **39**, pp. 1491–1507.

ZIRNIG, W., HAUSAMANN, D. and SCHREIER, G., 2002, High-resolution remote sensing used to monitor natural gas pipelines. *Earth Observation Magazine*, **3**, pp. 1–8.